

# A survey on snake robot modeling and locomotion

Aksel Andreas Transeth<sup>†\*</sup>, Kristin Ytterstad Pettersen<sup>‡</sup> and  
Pål Liljebäck<sup>‡</sup>

<sup>†</sup>*SINTEF ICT, Applied Cybernetics, NO-7465 Trondheim, Norway*

<sup>‡</sup>*Department of Engineering Cybernetics, Norwegian University of Science and Technology, O.S. Bragstadsplass 2D, NO-7491 Trondheim, Norway*

(Received in Final Form: January 27, 2009. First published online: March 3, 2009)

## SUMMARY

Snake robots have the potential to make substantial contributions in areas such as rescue missions, firefighting, and maintenance where it may either be too narrow or too dangerous for personnel to operate. During the last 10–15 years, the published literature on snake robots has increased significantly. The purpose of this paper is to give a survey of the various mathematical models and motion patterns presented for snake robots. Both purely kinematic models and models including dynamics are investigated. Moreover, the different approaches to biologically inspired locomotion and artificially generated motion patterns for snake robots are discussed.

**KEYWORDS:** Snake robots; Dynamics; Kinematics; Locomotion.

## 1. Introduction

The wheel is an amazing invention, but it does not roll everywhere. Wheeled mechanisms constitute the backbone of most ground-based means of transportation. On relatively smooth surfaces, such mechanisms can achieve high speeds and have good steering ability. Unfortunately, rougher terrain makes it harder, if not impossible, for such mechanisms to move. In nature, the snake is one of the creatures that exhibits excellent mobility in various types of terrain. It is able to move through narrow passages and climb on rough ground. This property of mobility is attempted to be recreated in robots that look and move like snakes. Snake robots usually have a high number of degrees of freedom (DOF) and they are able to move without using active wheels or legs.

Snake robots may one day play a crucial role in search and rescue operations, firefighting, and inspection and maintenance. The highly articulated body allows the snake robot to traverse difficult terrains such as collapsed buildings or the chaotic environment caused by a car collision in a tunnel. The snake robot could crawl through destroyed buildings looking for people, while simultaneously bringing communication equipment together with small amounts of food and water to anyone trapped in the shattered building. A rescue operation involving a snake robot has been envisioned

by Miller.<sup>1</sup> Moreover, the snake robot can be used for surveillance and maintenance of complex and possibly hazardous areas of industrial plants such as nuclear facilities. In a city, it could inspect the sewerage system looking for leaks or aiding firefighters. Also, snake robots with one end fixed to a base can be used as a robot manipulator which can reach hard-to-get-to places.

Compared to wheeled and legged mobile mechanisms, the snake robot offers high stability and good terrainability. The exterior can be completely sealed to keep dust and fluids out. Due to high redundancy and modularity, the snake robot is robust to mechanical failure. The downside is its limited payload capacity, poor power efficiency, and a very large number of DOF that have to be controlled.

The first qualitative research on snake locomotion was done by Gray in 1946.<sup>2</sup> The first working biologically inspired serpentine robot was constructed by Hirose in 1972.<sup>3</sup> He presented a 2-m long serpentine robot with 20 revolute 1-DOF joints called the Active Cord Mechanism model ACM III shown in Fig. 1. Passive casters were put on the underside of the robot. Forward motion was obtained by moving the joints to the left and right in selected patterns.

Since Hirose presented his Active Cord Mechanism, many multi-link articulated robots intended for crawling locomotion have been developed and have had many names. Some examples are multi-link mobile robot,<sup>4</sup> snake-like or snake robot,<sup>5–11</sup> hyper-redundant robot,<sup>12</sup> and G-snake.<sup>13</sup> To emphasize that this paper deals with robots that mainly resemble the locomotion of snakes, the term “snake robot” will be employed. The snake robots referred to in this paper are implemented either with passive wheels<sup>3,4,14,15</sup> or without wheels.<sup>16–21</sup> The joints are mostly revolute, but extensible (prismatic) joints are also employed.<sup>17,22</sup>

Motion patterns of snakes, inchworms, and caterpillars are used as an inspiration about how the snake robots should move. Mathematical models of the snake robots are needed to analyze the motion patterns and to simulate their motion. Because of the high number of DOF, the construction of such models is a challenge. During the last 10–15 years, the literature published on snake robots has increased significantly, and the purpose of this paper is to provide a concise overview and comparison of the various mathematical models and locomotion principles of snake robots presented during this period. The relationship between

\* Corresponding author. E-mail: Aksel.A.Transeth@sintef.no

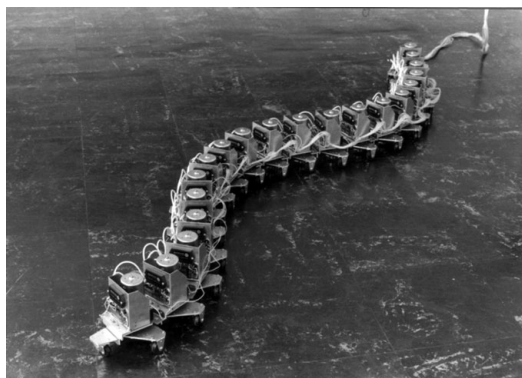


Fig. 1. The Active Cord Mechanism model ACM III.<sup>3</sup> By permission of Oxford University Press.

snake robot design and the choice of gait is outlined, and some recent results on locomotion patterns are given. We also provide an introduction to the source of inspiration of snake robots: biologically inspired crawling locomotion. In addition, we mention some possibly advantageous biological motion patterns which are not yet implemented for snake robots. A number of biologically inspired motion patterns implemented on snake robots are presented. Moreover, other useful motion patterns that are not directly associated with biological creatures are described. Selected mathematical models will be presented more thoroughly. The specific choices of hardware for sensors and actuators is beyond the scope of this paper and will not be discussed.

This paper is arranged as follows: Section 2 gives a short introduction to snakes and biological, crawling locomotion. Various mathematical models of snake robots are presented in Section 3. Section 4 provides an overview of numerous motion patterns implemented on snake robots, while the results presented in this paper are discussed and future research is suggested in Section 5. Concluding remarks are given in Section 6.

## 2. Biological Snakes and Inchworms

The physiology of biological snakes, inchworms, and caterpillars is an important source of inspiration for researchers developing mathematical models and control strategies for snake robots. This section therefore provides a short introduction to snake physiology and snake locomotion. In addition, inchworm and caterpillar motion patterns are outlined. Unless otherwise specified, the content in this section is based on the work by Mattison,<sup>23</sup> Bauchot,<sup>24</sup> and Dowling.<sup>25</sup> A short discussion of the connection between the contents in this section and snake robot modeling and locomotion is given at the end of this section. A more thorough description of this relationship is given in Sections 3 and 4.

### 2.1. Snake skeleton

The skeleton of a snake often consists of at least 130 vertebrae, and can exceed 400 vertebrae. The range of movement between each joint is limited to between  $10^\circ$  and  $20^\circ$  for rotation from side to side, and to a few degrees of rotation when moving up and down. A large total curvature

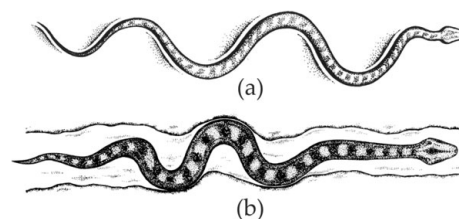


Fig. 2. (a) Lateral undulation and (b) concertina locomotion.<sup>23</sup> By permission of Cassell Illustrated.

of the snake body is still possible because of the high number of vertebrae.

A very small rotation is also possible around the direction along the snake body. This property is employed when the snake moves sideways by sidewinding.

### 2.2. Snake skin

Since snakes have no legs, the skin surface plays an important role in snake locomotion.<sup>24</sup> A snake should experience little friction when sliding forwards, but greater friction when pushed backwards. The skin is usually covered with scales with tiny indentations which facilitate forward locomotion. Moreover, an important property for forward locomotion with a gait called “lateral undulation” is that the scales form an edge to the belly during motion. This makes the friction between the underside of the snake and the ground higher transversal to the snake body compared to the friction in the direction along the body.<sup>3</sup>

**2.3. Locomotion—the source of inspiration for snake robots** Most motion patterns implemented for snake robots are inspired by the locomotion of snakes. However, inchworms and caterpillars are also used as an inspiration. The relevant motion patterns of all these creatures will be outlined here.

**2.3.1. Lateral undulation.** Lateral undulation (also termed as serpentine crawling) is a continuous movement of the entire body of the snake relative to the ground. Locomotion is obtained by propagating waves from the front to the rear of the snake while exploiting roughness in the terrain. Every part of the body passes the same part of the ground ideally leaving a single sinus-like track as illustrated in Fig. 2(a). To prevent lateral slipping while moving forward, the snake “digs” in to the ground with the help of the edge described in Section 2.2. In addition, it may use contours such as rocks on the ground to push against. All the contact points with the ground constitute push-points for the snake, and the snake needs at least three push-points to obtain a continuous forward motion. Two points are needed to generate forces. The third point is used to balance the forces such that they act forward.

The efficiency of lateral undulation is mainly based on two factors. (1) The contour of the ground. Contours in the ground increase the efficiency of the locomotion. (2) The ratio between the length of the snake and its circumference. The fastest snakes have a length that is no longer than 10–13 times their circumference. Speeds up to 11 km/h have been observed in rough terrain.

**2.3.2. Concertina locomotion.** A concertina is a small accordion instrument. The name is used in snake locomotion

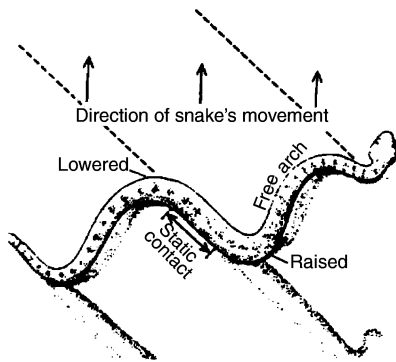


Fig. 3. Sidewinding locomotion<sup>26</sup> © 1993 IEEE.

to indicate that a snake stretches and folds its body to move forward. The folded part is kept in a fixed position while the rest of the body is either pushed or pulled forward as shown in Fig. 2(b). Then, the two parts switch roles. Forward motion is obtained when the force needed to push back the fixed part of the snake body is higher than the friction forces on the moving part of the body.

Concertina locomotion is employed when a snake moves through narrow passages such as pipes or along branches. If the path is too narrow compared to the diameter and curving capacity of a snake, the snake is unable to progress by this motion pattern.

**2.3.3. Sidewinding locomotion.** Sidewinding is probably the most astonishing gait to observe and is mostly used by snakes in the desert. The snake lifts and curves its body leaving short, parallel marks on the ground while moving at an inclined angle as shown in Fig. 3. Unlike lateral undulation, there is a brief static contact between the body of the snake and the ground.

Sidewinding is usually employed on surfaces with low shear such as sand. Snakes can reach velocities up to 3 km/h during sidewinding locomotion.

**2.3.4. Other snake gaits.** Snakes also have gaits that are employed in special situations or by certain species. These are for example rectilinear crawling, burrowing, jumping, sinus-lifting, skidding, swimming, and climbing. The latter four, which are or may be used for snake robots are as follows.

Sinus-lifting is a modification of lateral undulation where parts of the trunk are lifted to avoid lateral slippage and to optimize propulsive force.<sup>3</sup> This gait is employed for high speeds.

A variation of lateral undulation is called *skidding* (also termed as *slidepushing*) and is employed when moving past low-friction surfaces. The snake rests its head on the ground and then sends a flexion wave down through its body. This is repeated in a zigzag pattern and is a very energy-inefficient way of locomotion.

Almost all snakes can swim. They move forward by undulating laterally like an eel.

Long and thin bodied snakes can climb trees by vertical lateral undulation. Parts of their body hang freely in the air, while branches are used as support.

**2.3.5. Inchworm and caterpillar locomotion.** An inchworm moves forward by grabbing the ground with its front legs

while the rear end is pulled forward. The rear legs then grab the ground and the inchworm lifts its front legs and straightens its body. Caterpillars send a vertical traveling wave through their body from the end to the front in order to move forward. Small legs give the necessary friction force while on the ground.

#### 2.4. Discussion of results in connection to snake robots

We see from the above content in this section that biological snakes are amazing creatures. They are able to move forward without legs or arms and they control several hundred joints simultaneously. We will see in the remainder of this paper that the snake body and its form of locomotion are used as an inspiration for how to model snake robots and how to make them move.

In Section 3, we deal with mathematical modeling of snake robots. These snake robots typically have somewhere between 5 and 20 DOF. This is significantly lower than around 400 vertebrae of a biological snake. However, the cost and difficulty of building a snake robot with that many joints would be substantial. Moreover, the high number of DOF would increase the complexity of a mathematical model of the snake robot considerably. Therefore, snake robots are generally designed with fewer joints than those for biological snakes, but with large allowable joint angles so that the snake robot is still somewhat able to mimic the flexibility of a biological snake.

In Section 4, we discuss various forms of snake robot locomotion. We will see that lateral undulation is a gait often adopted from real snakes. Sidewinding is another frequently used gait. However, sidewinding requires that a snake robot is capable of vertical motion in addition to horizontal motion. This has consequences for both the design of the snake robot and the mathematical model.

### 3. Mathematical Modeling

This section provides an overview of previous work concerning modeling of the kinematics and dynamics of a snake robot. Many approaches and results are found in the literature. Some work focuses on both the kinematics and the dynamics of the snake robot, while others focus only on the kinematics. Snake robots may be categorized through certain basic properties: (1) type of joints, (2) number of degrees of freedom, and (3) with or without wheels. Most snake robots consist of links connected by revolute joints with 1 or 2 DOF. On some robots, the links are extensible (i.e. prismatic joints). To achieve the desired frictional property for lateral undulation mentioned in Section 2, some snake robots are equipped with passive wheels. When wheels are employed, the dynamics of the interaction between the robot and the ground surface is often ignored. If no wheels are attached, this friction force needs to be considered for some, but not all, gaits (see Section 4). The use of passive wheels or not along the snake robot body is an important property that will be employed throughout this section in order to categorize the various mathematical models.

This section consists of two parts. Section 3.1 presents approaches aimed at modeling the kinematics of snake robots, while Section 3.2 presents various dynamic models.

Wheeled and wheel-less robots are sometimes treated in separate sections here. This is because the friction force between the ground and the snake robot is most often not modeled for snake robots with passive wheels. Instead, contact with the ground surface is typically described by kinematic relationships such as nonholonomic constraints (see Section 3.1.2). However, it is important to note that the general methods presented for describing the dynamics and kinematics of snake robots with and without wheels are the same (e.g. the Denavit–Hartenberg convention, the Lagrangian formulation, and the Newton–Euler formulation). As previously mentioned, the difference lies in the description of the contact with the ground surface. Sometimes this contact model is incorporated into the general model of the snake robot, thus giving a different final model (with, e.g. less DOF). Hence, this is the motivation for separating wheeled and wheel-less snake robots in the later description of the models.

It is emphasized that design issues for snake robots are not the focus of this paper, but are included where these issues affect the modeling approach taken in the referred work.

### 3.1. Kinematics

The kinematics describes the geometrical aspect of motion. Different modeling techniques ranging from classical methods such as the Denavit–Hartenberg (D-H) convention (see, e.g. the book by Murray *et al.*<sup>27</sup> for more on the D-H convention) to specialized methods for hyper-redundant structures (structures with a high number of DOF) have been employed. The following subsections will elaborate on the different modeling techniques.

**3.1.1. The Denavit–Hartenberg convention.** The D-H convention is a well-established method for describing the position and orientation of the links of a robot manipulator with respect to a (usually fixed) base frame. Different solutions are presented that deal with the fact that the base of a snake robot is not fixed.<sup>28,29</sup>

Poi *et al.*<sup>28</sup> present a snake robot consisting of nine equal modules. Each module consists of seven revolute 1-DOF joints which are connected by links of equal length. Three joints and four joints have the axis of rotation perpendicular to the horizontal and vertical plane, respectively. Each module is parameterized with the D-H convention. A modification to the convention has been proposed by placing the base coordinate system on the first motionless link of the part of the structure which is in motion. Hence, the links in motion are described in an inertial frame. The snake robot described by Poi *et al.*<sup>28</sup> moves only four or five modules simultaneously, so giving the position and orientation relative to the first motionless link prevents traversing through the complete structure to obtain positions and orientations in an inertial frame.

The motion patterns employed in a work by Liljebäck *et al.*,<sup>29</sup> sidewinding and lateral undulation, are based on constant joint movement, so we have to traverse through the whole structure and hence the previously presented approach<sup>28</sup> will not simplify the mathematical structure. Therefore, a *virtual structure for orientation and position* (VSOP) is introduced to be able to describe the kinematics

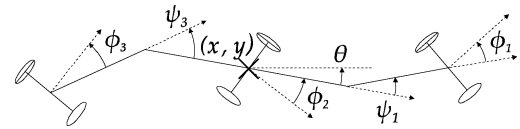


Fig. 4. The first three links of the ACM III employed by Ostrowski and Burdick.<sup>14</sup>

of the snake robot in an inertial reference frame. Liljebäck *et al.*<sup>29</sup> present a snake robot with five revolute 2-DOF joints. The VSOP describes the trailing link of the snake robot in an inertial reference frame by three orthogonal prismatic joints and three orthogonal revolute joints which represent the position and orientation, respectively. These virtual joints are connected by links with no mass. By employing the VSOP in the D-H convention, the position and orientation of each joint is given in an inertial coordinate system.

**3.1.2. Nonholonomic constraints and snake robots with passive caster wheels.** The key to snake robot locomotion is to continuously change the shape of the robot. This is achieved by rotation and/or elongation of its joints. Krishnaprasad and Tsakiris<sup>13</sup> and Ostrowski and Burdick<sup>14</sup> both present kinematic approaches on how to link the changes in internal configuration to the net position change of the robot. The relation is found by utilizing nonholonomic constraints (which arise from having wheels on the snake robot) and differential geometry such as connections. Ostrowski<sup>14</sup> employs Hirose’s Active Cord Mechanism Model 3 (ACM III) as an example which will be explained here. The first three pairs of wheels of ACM III are illustrated in Fig. 4. The five joint angles  $\phi_1$ ,  $\phi_2$ ,  $\phi_3$ ,  $\psi_1$ , and  $\psi_3$  are controlled inputs. The kinematic nonholonomic constraints are realized by adding passive caster wheels on the snake robot and may be written in the form

$$\dot{x}_i \sin(\phi_i) - \dot{y}_i \cos(\phi_i) = 0, \quad (1)$$

where  $(\dot{x}_i, \dot{y}_i)$  is the velocity of the center of mass and  $\phi_i$  is the angle of the joint to which the wheels are attached. More information on nonholonomic systems is given by Kolmanovsky and McClamroch<sup>30</sup> and Bloch *et al.*<sup>31</sup> The wheels are assumed not to slip and therefore realize an ideal version of the frictional properties of the snake skin as mentioned in Section 2.2.

A *local form*  $\mathbb{A}$  of a *connection* provides the following relation between the shape changes of the snake robot and its net locomotion:

$$g^{-1} \dot{g} = -\mathbb{A}(r) \dot{r}, \quad (2)$$

where  $r$  is the shape variables and  $g \in SE(2)$  gives the overall position and orientation of the snake robot.<sup>14</sup> The connection provides understanding of how shape changes can generate locomotion and can even be used for controllability tests.<sup>32</sup> The simple form of Eq. (2) is dependent on the kinematic constraints breaking all the symmetries of the Lagrangian function which may raise dynamic constraints. This is achieved, with the ACM III as an example by using the first three segments to define the net motion of the snake robot. These segments define the path which is to be

followed by the remaining segments due to the nonholonomic constraints on the wheels.

This modeling technique has also been used to include the dynamics, this is described in Section 3.2.2.

**3.1.3. Backbone curves and continuum robots.** Instead of starting by finding the position and orientation of each joint directly as with the D-H convention, a curve that describes the shape of the “spine” of the snake robot can be employed.<sup>12,33–36</sup> The Frenet–Serret apparatus<sup>37</sup> is employed in a classical handling of the geometry of curves.<sup>12</sup> However, this approach has some limitations.<sup>12</sup> First, the Frenet–Serret frames assigned along the curve are not defined for straight line segments. Second, the vector function describing the spatial curve requires a numerical solution of a cumbersome differential equation. The introduction of backbone curves (see, e.g. ref. [12]) is a way of handling these limitations. The backbone curve is defined as “a piecewise continuous curve that captures the important macroscopic geometric features of a hyper-redundant robot”<sup>12</sup> and it typically runs through the spine of the snake robot. A set of orthonormal reference frames are found along the backbone curve at a set of “fitting” points in order to specify the actual snake robot configuration. The backbone curve parametrization together with an associated set of orthonormal reference frames is called a *backbone curve reference set*.<sup>33,35</sup>

The problem of determining joint angles of a robot manipulator given the end-effector position is called the inverse kinematics problem. For hyper-redundant manipulators (such as snake robots) there will generally be an infinite number of solutions due to the redundant number of DOF. When the backbone curve concept is employed, the problem is reduced to determining the proper time-varying behavior of the backbone reference set.<sup>35</sup> Once the backbone reference set is determined, a fitting procedure may be employed in order to align the manipulator with the backbone curve. A modal decomposition approach was taken by Chirikjian and Burdick in order to control the backbone curve to which a manipulator is fitted.<sup>12</sup> The work presents “fitting” algorithms that position the end-effector of the manipulator in exact correspondence with the continuous backbone curve shape, while the rest of the manipulator approximately adheres to the backbone curve.

A more recent work by Wang and Chirikjian presents an alternative approach to the inverse kinematics problem of a hyper-redundant manipulator.<sup>38</sup> The work presents a diffusion-based algorithm for calculating the workspace of a manipulator based on its workspace density (defined as the density of reachable points/frames in any portion of the workspace). The calculated workspace density is then employed in order to solve the inverse kinematics algorithm by configuring the manipulator to achieve maximum workspace density around the target spot.

Another recent alternative approach to the methods presented by Chirikjian and Burdick<sup>12,33</sup> has been given by Yamada and Hirose.<sup>36</sup> This approach is called the bellows model and is specifically designed for separating explicitly between twisting and bending of the body of a snake robot. This is advantageous since most snake robots are designed

with joints capable of bending, but not twisting (for example snake robots with cardan joints). Hence, the ability to twist can simply be left out of the model of the snake robot. None of the literature has published work on how to fit the continuous bellows model to a physical snake robot with a discrete morphology.

Continuum robots are a special type of flexible manipulators in that they do not contain rigid links and identifiable rotational joints.<sup>39</sup> The biological counterparts of these mechanisms are found in nature in the form of e.g. elephant trunks, octopus arms, and squid tentacles. The Slim Slime robot developed by Hirose<sup>17</sup> is an example of a continuum robot developed for locomotive purposes. The continuous backbone curve concept may be employed in order to model a continuum robot. However, the modal decomposition approach taken by Chirikjian and Burdick<sup>12</sup> relies on approximating the shape of the actual robot. A method for calculating the exact kinematics of trunk sections of a continuum robot has been developed by Jones and Walker.<sup>40</sup> The approach is modular and thereby applicable to a wide range of physical realizations of the manipulator. The forward kinematics of the continuum robot is established through multiple steps. First, the state of the actuators in each trunk section (e.g. the length  $l$  of the actuator cables or the pressure  $p$  of the pneumatic actuators) is converted to the kinematic parameters  $s$ ,  $\kappa$ , and  $\phi$  of the trunk section, where  $s$  is the trunk length,  $\kappa$  determines curvature, and  $\phi$  determines the angle of curvature. Next, based on the work by Hannan and Walker,<sup>41</sup> the kinematic parameters  $s$ ,  $\kappa$ , and  $\phi$  for each trunk section are converted to conventional D-H parameters  $\theta$  and  $d$  (see Section 3.1.1) by fitting a conceptual rigid-link manipulator to the continuous backbone of the trunk section. Finally, the D-H convention is used to compute the trunk tip position and orientation.

Additional work related to the kinematics of continuum robots has been presented by Gravagne and Walker.<sup>42,43</sup> The work discusses issues around the kinematic model and presents mappings between the continuum manipulator shapes and the finite-dimensional actuator space. The kinematics of continuum robots has also been studied by Mochiyama and Kobayashi.<sup>44–46</sup> The authors have studied kinematic properties of continuum robots and examined the shape correspondence between a hyper-redundant robot and a desired spatial curve.

### 3.2. Dynamics

The dynamics of the snake robots presented has been derived by utilizing various modeling techniques such as the Newton–Euler formulation, the Lagrangian formulation, and geometric mechanics.

For snake robots without wheels, the friction between the snake robot and the ground affects the motion of the snake robot significantly. Thus, for these snake robots, the dynamics should be modeled for locomotion patterns such as lateral undulation. For snake robots with wheels, however, the wheels greatly reduce the friction in the longitudinal direction and, hence, make it possible to use a purely kinematic model of the robot by assuming nonslip conditions. The majority of the results presented on the modeling of the dynamics have therefore considered snake robots without wheels. Here, we

will first give a short introduction to some of the notation used later, then we give a brief overview of a selection of the results reported on the modeling of dynamics of wheeled snake robots, and finally we present the results on snake robots without wheels. It is important to note that the modeling techniques presented for wheel-less snake robots can also be utilized to describe the dynamics of wheeled snake robots. However, the friction coefficients or sometimes even the entire friction model will be different.

To ease the presentation of the mathematical models, a common notation for some of the material is presented which is based on part of the work by Prautsch and Mita<sup>47</sup> and Saito *et al.*<sup>19</sup> Denote the mass  $m_i$ , length  $2l_i$ , and moment of inertia  $J_i$  for each link,  $i = 1, 2, \dots, n$ . The snake robot moves in the  $xy$ -plane. Denote the angle  $\theta_i$  between link  $i$  and the inertial (base)  $x$ -axis. Denote position of the center of gravity (CG) of link  $i$  by  $(x_i, y_i)$ . Denote the unit vectors tangential  $\mathbf{e}_t^{B_i} \in \mathbb{R}^2$  and normal  $\mathbf{e}_n^{B_i} \in \mathbb{R}^2$  to the link  $i$  in the horizontal  $xy$ -plane. Hence,  $\mathbf{e}_t^{B_i}$  points along link  $i$  and  $\mathbf{e}_n^{B_i} \perp \mathbf{e}_t^{B_i}$ . Denote the velocity  $\mathbf{v}_i = [\dot{x}_i \ \dot{y}_i]^T \in \mathbb{R}^2$  of link  $i$ , and tangential and normal velocity of link  $i$   $\mathbf{v}_{i,t} = \mathbf{e}_t^{B_i} (\mathbf{e}_t^{B_i})^T \mathbf{v}_i$  and  $\mathbf{v}_{i,n} = \mathbf{e}_n^{B_i} (\mathbf{e}_n^{B_i})^T \mathbf{v}_i$ , respectively.

The friction forces that act on the CG of link  $i$  are denoted by  $\mathbf{f}_i = [f_{x_i} \ f_{y_i}]^T \in \mathbb{R}^2$  where  $f_{x_i}$  and  $f_{y_i}$  are friction forces between link  $i$  and the ground along the  $x$ - and  $y$ -directions of the inertial frame, respectively. The coefficients of friction tangential and normal to link  $i$  are  $c_{i,t}^{(j)}$  and  $c_{i,n}^{(j)}$ , respectively, where  $j$  is used in this paper to distinguish between the coefficients in the various friction models.

**3.2.1. Snake robots with passive caster wheels.** A desired property for moving by the serpentine motion pattern lateral undulation is to keep the difference between lateral and longitudinal friction as high as possible. This property of friction can be obtained by attaching caster wheels to the belly of the snake robot. The equations of motion of a simplified version of the snake robot used by Hirose<sup>3</sup> are presented by Prautsch and Mita.<sup>47</sup> The robot is the same as the ACM III shown in Fig. 1 except that the wheel axles are fixed. The dynamic model is derived to utilize acceleration-based control algorithms. It is assumed that the wheels do not slip sideways.

A snake robot (called the SR#2) has been presented and compared to the ACM III by Wiriyacharoensunthorn and Laowattana.<sup>4</sup> The ACM model assumes that the wheels do not slip. This nonslippage introduces nonholonomic constraints. The SR#2 model is based on *holonomic* framework and is hence without the no-slip condition. The argument used against assuming no slip is that it is difficult to control the torques in the joints such that the assumption is satisfied. Simulations show that the ACM III build up an error in position while following a circular path. This is not the case for SR#2, something which makes it a more accurate model for this scenario.

The above models have all described planar motion. However, a 3D model of the dynamics of a snake robot with wheels that do not slip has also been presented.<sup>48</sup> In addition, a system equation for the control of the height of the wheels is given and computer simulations are presented.

**3.2.2. Snake robots without wheels.** The use of wheels may decrease terrainability,<sup>19</sup> thus wheel-less robots may have an advantage. As discussed earlier, friction plays a significant role for wheel-less snake robots. Hence, it is necessary to model the dynamics and not only the kinematics for relatively high speeds of motion. This subsection first provides an overview of friction models developed for snake robots. Subsequently, a selection of dynamic models derived for snake robots without wheels will be presented. As previously mentioned, these models can also be applied for wheeled snake robots. However, particular assumptions can be made that simplify the model of such robots significantly as described above.

*Friction and contact models:* The friction models presented in literature on snake robots are based on a Coulomb or viscous-like friction model and such models are explained, for instance, in the book by Egeland and Gravdahl.<sup>49</sup> For 3D models of snake robots, it is necessary to model the normal contact force due to impacts and sustained contact with the ground, in addition to the friction force. This force has been described as compliant by a spring-damper model in Liljebäck *et al.*<sup>29</sup> as

$$f_{N_i} = \begin{cases} 0 & , z_i \geq 0 \\ -k \cdot z_i - d \cdot \dot{z}_i & , z_i < 0, \end{cases} \quad (3)$$

where  $z_i \in \mathbb{R}$  is the height of the CG of link  $i$ ,  $\dot{z}_i = \frac{dz_i}{dt}$ ,  $k \in \mathbb{R}^+$  is the constant spring coefficient of the ground, and  $d \in \mathbb{R}^+$  is a constant damping coefficient that serves to dampen the oscillations induced by the spring. Using  $f_{N_i}$ , the friction force on link  $i$ , based on a simple, viscous-like model, is written as

$$\mathbf{f}_i = -c_{i,t}^{(1)} f_{N_i} \mathbf{v}_{i,t} - c_{i,n}^{(1)} f_{N_i} \mathbf{v}_{i,n} \in \mathbb{R}^2. \quad (4)$$

The sum of forces acting on link  $i$  in the model presented by Liljebäck<sup>29</sup> is  $\mathbf{f}_i^{3D} = [\mathbf{f}_i^T \ f_{N_i}]^T \in \mathbb{R}^3$ . The spring coefficient  $k$  needs to be set very high to imitate a solid surface. Hence, the total system is stiff and requires a very small simulation step size to be simulated. However, the constitute law (3) for the normal force provides an intuitive and simple approach to implementing the normal force. A friction model including both static and dynamic friction properties for a 3D dynamic model is given by Ma *et al.*<sup>50</sup>

The 2D anisotropic viscous friction model used by Grabec<sup>20</sup> can be derived from (4) by setting  $f_{N_i} \equiv 1$ . In this case, the friction force is found from

$$\mathbf{f}_i = \mathbf{H}_i \mathbf{v}_i, \quad (5)$$

where

$$\mathbf{H}_i = c_{i,n}^{(2)} \left[ \left( 1 - \frac{c_{i,t}^{(2)}}{c_{i,n}^{(2)}} \right) \mathbf{e}_t^{B_i} (\mathbf{e}_t^{B_i})^T - \mathbf{I}_{2 \times 2} \right], \quad (6)$$

and  $\mathbf{I}_{2 \times 2} \in \mathbb{R}^{2 \times 2}$  is a unit matrix.

The effect of rotational motion of the links is introduced in the two 2D friction models, one with viscous and one with Coulomb friction, presented by Saito *et al.*<sup>19</sup> Both models

are derived by integrating the infinitesimal friction forces on a link. The translational part of the viscous friction model is given by Eq. (4) with  $f_{N_i} = m_i$  (i.e.  $f_{N_i}$  is not an actual force). The total viscous friction torque due to rotational velocity around the center of mass of link  $i$  is found to be

$$\tau_i = -c_{i,n}^{(3)} J_i \dot{\theta}_i \in \mathbb{R}, \quad (7)$$

For translational motion, the friction force based on Coulomb's law is found for  $\dot{\theta}_i = 0$  as<sup>19</sup>

$$\begin{aligned} \mathbf{f}_i = & -m_i g \begin{bmatrix} \cos \theta_i & -\sin \theta_i \\ \sin \theta_i & \cos \theta_i \end{bmatrix} \begin{bmatrix} c_{i,t}^{(3)} & 0 \\ 0 & c_{i,n}^{(3)} \end{bmatrix} \\ & \times \text{sign} \left( \begin{bmatrix} (\mathbf{e}_t^{B_i})^T \mathbf{v}_i \\ (\mathbf{e}_n^{B_i})^T \mathbf{v}_i \end{bmatrix} \right). \end{aligned} \quad (8)$$

The expression for the Coulomb friction force is slightly different for  $\dot{\theta}_i \neq 0$ .<sup>19</sup> However, we only include the case when  $\dot{\theta}_i = 0$  here to simplify the presentation. Employing Coulomb's law of dry friction as the friction model results in a more complicated, but also a more accurate model for motion on non-lubricated surfaces. Model (4) does not include dry friction and thus the high friction forces which may arise at low velocities are not modeled. Nevertheless, results from an analysis of the parameters governing the snake robot motion pattern during locomotion by lateral undulation were generally the same for the viscous and the Coulomb friction model.<sup>19</sup>

Recent results by Transeth *et al.*<sup>51,52</sup> on 3D modeling of snake robots show how to describe the normal contact forces with the ground, together with the Coulomb friction force in the framework of nonsmooth dynamics. The snake robot is then modeled as a hybrid system, and the change in velocity of a snake robot link hitting the ground surface is instantaneous. Hence, there is no need for the spring and damper coefficient in Eq. (4) since the ground contact force is modeled using a set-valued force law. In addition, the Coulomb friction force is modeled with a set-valued force law. The set-valuedness gives rise to a friction force that is different from zero when a link is subjected to a force while still at zero velocity due to the Coulomb friction (this is the stick-phase). This is not possible in a smooth framework when for example using the sign-function to describe the Coulomb friction since  $\text{sign}(0) = 0$ .

For most of the gaits simulated with the above friction models, the property  $c_{i,t} < c_{i,n}$  has been implemented to realize the anisotropic friction property of a snake moving using lateral undulation. It may be difficult to design a snake robot with  $c_{i,t} < c_{i,n}$  on a general surface. Sidewinding has been implemented with an isotropic friction model ( $c_{i,n} = c_{i,t}$ ) by Liljebäck *et al.*<sup>53</sup> and as a purely kinematic case by Burdick *et al.*<sup>26</sup> Special gaits for planar motion based on an isotropic friction model are detailed by Chernousko.<sup>54,55</sup>

*Dynamic model with decoupling:* A five-link snake robot with 1-DOF joints is modeled and controlled by Saito *et al.*<sup>19</sup> The robot is built and experiments performed to validate the theoretical results. Metal skates are put on the belly to implement the anisotropic friction property  $c_{i_t} < c_{n_i}$ .

The dynamic model of the snake robot is developed from the Newton–Euler equations resulting in two sets of equations: one for translational motion of the center of mass  $\mathbf{w}$  of the snake robot and another for the rotational motion of the angle of each link given in an inertial frame. The final equations of motion can be decoupled into two parts: shape motion and inertial locomotion. The shape motion maps the joint torques to joint angles while the inertial locomotion relates the joint angles to the inertial position and orientation. This simplifies the analysis and synthesis of locomotion of the snake robot. To achieve decoupling, a vector of relative angles  $\boldsymbol{\phi} \in \mathbb{R}^{n-1}$ , where the  $i$ th element of  $\boldsymbol{\phi}$  is  $\phi_i = \theta_i - \theta_{i+1}$ , and a quantity  $\dot{\psi} \in \mathbb{R}$  which can be thought of as “an average angular momentum” are introduced.<sup>19</sup> The expressions for shape motion and inertial motion, respectively, are found to be

$$\mathbf{h}_s(\ddot{\boldsymbol{\phi}}, \boldsymbol{\theta}, \dot{\boldsymbol{\theta}}, \dot{\mathbf{w}}) = \mathcal{B}\mathbf{u}, \quad (9)$$

$$\mathbf{h}_i(\dot{\psi}, \ddot{\psi}, \boldsymbol{\theta}, \dot{\mathbf{w}}, \ddot{\mathbf{w}}, \dot{\boldsymbol{\phi}}) = 0, \quad (10)$$

where  $\mathbf{h}_s(\cdot)$ ,  $\mathbf{h}_i(\cdot) \in \mathbb{R}^n$  are functions,<sup>19</sup>  $\boldsymbol{\theta} = [\theta_1 \dots \theta_n]$ ,  $\mathbf{u}$  are the joint torques and  $\mathcal{B}$  is an invertible matrix. Control of the snake robot is now performed in two steps. First, the joint torques  $\mathbf{u}$  control the shape of the robot and second the relative angles  $\boldsymbol{\phi}$  control the average angular momentum  $\dot{\psi}$  and position  $\mathbf{w}$ . For someone who needs a 2D model of a snake robot and has a basic knowledge of classical mechanics, this is probably the easiest 2D model to implement for simulation due to the concise and comprehensive presentation of the model in the paper.

*Quasi-stationary equations of motion:* A 2D model based on the Newton–Euler formulation of a snake robot with 1-DOF revolute joints with the viscous friction model (5) is presented by Grabec.<sup>20</sup>

Non-dimensional variables are introduced to simulate the dynamics of the snake robot. The resulting system of second-order nonlinear equations which constitute the non-dimensional model of the snake robot may become unstable during simulation. To aid the numerical treatment, overcritical damping is introduced by setting accelerations to zero. The result is a set of quasi-stationary first-order differential equations of motion. By employing the first-order equation for translational motion together with the friction model in short form (5) the velocity of the head of the snake robot is found to be

$$\mathbf{v}_{\text{head}} = - \left( \sum_{i=1}^n \mathbf{H}_i \right)^{-1} \sum_{i=1}^n \mathbf{H}_i \mathbf{v}_i^{(\text{rel})}, \quad (11)$$

where  $\mathbf{v}_i^{(\text{rel})}$  is the velocity of link  $i$  with respect to the head and  $\mathbf{H}_i$  is found from (6). Saito *et al.*<sup>19</sup> gives the relationship between shape changes from joint angle deflection and the position of the CG of the snake robot (10). To investigate locomotion analytically, (11) provides an alternative approach where the direct connection between velocities of each link relative to head of the snake robot and the head velocity is given.

*Creeping on a inclined plane:* A model of a snake robot with  $n$  links and 1-DOF rotational joints has been developed

from the Newton–Euler equations by Ma *et al.*<sup>18</sup> The actual snake robot that is modeled has wheels, however, the friction between the underside of the snake robot and the ground surface is modeled as anisotropic Coulomb friction. Hence, the wheels do not constitute nonholonomic constraints (i.e. the wheels may slip) and that is why we have included the model in this section. The model of planar motion of the snake robot is extended to motion on an inclined plane where the angle of inclination affects the motion of the snake robot.<sup>15,56</sup>

The mathematical model is presented in two ways (both for planar motion and the motion on an inclined plane). The first alternative is to write the model in a form where it is assumed that the joint angles together with the joint angle velocities and accelerations are given (shape-based control). From the specified data, the rotational and translational accelerations of the first link can then be found from the model. Thus, the motion of the snake robot in the plane is found. Moreover, the joint torques necessary to move the joint in the predetermined way can be found from the model. Hence, it is possible to study the joint torques and how they change for a specified motion pattern for various friction scenarios.

The second alternative is most common for snake robot models: how does the snake robot move given the commanded joint torques? By specifying the joint torques, the link angle accelerations are found. Then, the translational and rotational accelerations of the first link can be found, and the necessary velocities and positions are found by integration.

Simulation results are given for both shape-based and torque-based control of the snake robot.

*The Lagrangian:* Research on robots that resemble snakes is not only limited to land-based locomotion. Papers regarding anguilliform (eel-like) locomotion have also been published.<sup>21,57–59</sup> A five-link 2D snake robot (called the REEL II) with 1-DOF revolute joints, which will be used as an example, has been modeled and experimented with by McIsaac and Ostrowski.<sup>21</sup> Motion planning for such a robot consists of first building up the momentum to the snake robot and then steering the robot to its desired location. Hence, it is convenient that the mathematical model includes an explicit expression for the momentum. The model is formulated from the Lagrangian of the system and is summarized here.

The fact that the energy of the system and the frictional forces acting on the system are invariant with respect to the position and orientation of the snake robot (the system exhibits Lie groups symmetries) is exploited to simplify the mathematical model. The assumption that the joint angles are controlled directly (the same as saying that the dynamics (9) is ignored) yield two sets of resulting equations. The first equation relates the velocity of the snake robot to its internal shape changes and is similar to Eq. (2) given in Section 3.1.2 except for the locked inertia tensor  $\mathbb{I}(r)$  and generalized momentum vector  $p$  that have been added (we have a case of mixed constraints with both kinematic and dynamic constraints). The dynamics of the system is described by the generalized momentum equation which

is the second set of resulting equations. The generalized momentum  $p$  is associated with the momentum along the directions allowed by the kinematic constraints. A thorough explanation of the equations is given by Bloch *et al.*<sup>60</sup>

*Newton–Euler algorithm:* A physical and mathematical model of a snake robot with five 2-DOF joints is presented by Liljebäck *et al.*<sup>29</sup> In addition to the actual snake robot, a *virtual structure of orientation and position* (VSOP, see Section 3.1.1) is included in the dynamic model. The VSOP together with the snake robot have generalized minimal coordinates  $q \in \mathbb{R}^{2(n-1)+6}$  and generalized forces  $\tau \in \mathbb{R}^{2(n-1)+6}$ . The Newton–Euler formulation and the VSOP perspective is employed, and the dynamic model is written as

$$\mathbf{M}(q)\ddot{q} + \mathbf{C}(q, \dot{q})\dot{q} + \mathbf{g}(q) = \tau + \tau_{\text{ext}}, \quad (12)$$

where  $\mathbf{M}$  is the inertia matrix,  $\mathbf{C}$  is the Coriolis and centripetal matrix,  $\mathbf{g}(\cdot)$  is the vector of gravitational forces and torques, and  $\tau_{\text{ext}}$  is the vector including the external forces (friction and normal contact force). The matrices are detailed in another work by Liljebäck.<sup>53</sup> The Newton–Euler algorithm has been employed to simulate the snake robot. Hence, the full analytical expressions for the system matrices do not need to be found explicitly. Instead, the necessary matrices and accelerations are found numerically with the recursive Newton–Euler algorithm. This is advantageous since the analytical expressions for the system matrices are extremely large for a large number of joints when minimal coordinates are employed. For a model with non-minimal coordinates,<sup>50</sup> analytical expressions for the joint torques and head configuration of a 3D snake robot model deduced from the Newton–Euler equations are shown.

The Lagrangian and the Newton–Euler method are similar for rigid body dynamics in that the equations of motion obtained from the Lagrangian formulation are found by running through the Newton–Euler algorithm once.<sup>49</sup>

A modification of the Newton–Euler algorithm has been presented by Boyer *et al.*<sup>61</sup> to numerically evaluate a model of a *continuous* 3D underwater snake robot where the modeling approach is based on beam theory.

*Nonsmooth dynamics:* A nonsmooth (hybrid) 3D model of a snake robot with 10 2-DOF joints has been developed by Transth *et al.*<sup>51</sup> and external obstacles that the snake robot can push against for propulsion have been added to the model.<sup>52</sup> In addition, an experimental validation of a 2D version of the model with obstacles has been presented by Transth *et al.*<sup>62</sup> A specific choice of nonminimal coordinates yields a constant mass matrix which is advantageous for numerical treatment since the mass matrix needs to be inverted for each integration step. The changes in velocities due to impacts between the snake robot and the ground floor or the obstacles are modeled as instantaneous. The resulting contact forces are modeled with set-valued force laws. The set-valued force law for the normal force due to ground impact does not require that a spring and damper coefficient need to be determined as in Eq. (4). Instead, the collisions between the snake robot and the ground surface or the obstacles are modeled as completely inelastic by Transth *et al.*<sup>51,52,62</sup> The resulting equations that govern the motion of

the snake robot are found from the Newton–Euler equations, and the normal contact forces and friction forces are found from a transformation of the set-valued force laws.

*Continuum dynamics:* The concept of continuum robots was presented in Section 3.1.3. A computationally efficient scheme for the approximate calculation of the dynamics of a hyper-redundant robot has been presented by Chirikjian.<sup>35,63</sup> The method approximates the actual manipulator structure with a continuum structure based on the backbone curve model described in Section 3.1.3. The manipulator dynamics is calculated by “projecting” the dynamics of the continuum model onto the physical robotic structure. More specifically, the forces in the physical manipulator are matched with the forces in the continuum model. The forces in the continuum model are found from closed-form integrals that can be computed separately for each joint segment of the manipulator.

Mochiyama and Suzuki have also presented results on dynamic modeling of continuum robots.<sup>64–66</sup> Some of the work is similar to the work of Chirikjian presented earlier in that the backbone curve concept is employed,<sup>64</sup> but alternative perspectives and model representations are also presented.

Gravagne *et al.* have presented a model of the dynamics of a planar continuum robot with a spring-steel backbone.<sup>67</sup> The model is based on energy formulations of the spring-steel manipulator, and describes the large-deflection dynamics of the manipulator.

A study on the dynamics of elephant trunks has been presented by Wilson *et al.*<sup>68</sup> The work presents a model which approximates the stiffness of an elephant trunk in relation to the payload lifted by the trunk. The results target the description of elephant trunk dynamics, but are nevertheless interesting in a more general continuum manipulator perspective.

#### 4. Snake Robot Locomotion

A variety of approaches on how to make a snake robot move have been proposed. In most of the motion patterns or “gaits” used for locomotion, we find a distinct resemblance to the undulating locomotion of biological snakes or worms as described in Section 2. However, the motion patterns may be altered to compensate for the fact that the snake robots do not have exactly the same anatomy as biological snakes, inchworms, or caterpillars. For example, the snake robots

are not as articulated as their biological counterpart. This reduces moveability. In addition, snakes use their skin to sense external contact forces. A similar fine grid of sensors is difficult to implement on a snake robot.

Early studies of snake locomotion were given by Gray.<sup>2</sup> Later, a mathematical description of the serpentine motion of snakes was presented by Hirose.<sup>3</sup> An overview of the most frequent gaits that have been implemented on snake robots is found in Table I, and we see that lateral undulation is the most common motion pattern. We do not consider snake robots with *active* wheels in this paper. Examples of such snake robots are given in the papers by Kamegawa,<sup>11</sup> Yamada and Hirose,<sup>69</sup> and Masayuki *et al.*<sup>70</sup>

A description of a number of different motion patterns both for planar and 3D motion is given here.

##### 4.1. Planar snake robot locomotion

Planar snake robot locomotion is usually performed with the motion pattern lateral undulation. First, we present how to describe the motion pattern for a snake robot. Then, some examples are given together with other gaits for planar locomotion.

*4.1.1. The serpenoid curve.* A biological snake that moves by lateral undulation across a uniform surface displays a periodic creeping motion. The shape of the snake during this kind of locomotion has been studied by Hirose,<sup>3</sup> and he has presented the “serpenoid curve” as a way of describing the form of the gliding motion of a snake. The serpenoid curve is interesting for snake robot locomotion since the snake robot can move forward by moving its joints such that its body follows the trace of the serpenoid curve. The curve ensures that the curvature changes smoothly along the body, which is natural considering the contraction and relaxation of the muscles in a snake during locomotion.<sup>3</sup>

The serpenoid curve is shown in Fig. 5 and is a function of the distance  $s$  along the curve, the length  $l$  of one quarter period of the curve, and the winding angle  $\alpha_s(s, l)$  along the curve. Denote the tangential  $c_{i,t}$  and normal  $c_{i,n}$  frictional coefficient, between link  $i$  and the ground. The winding angle  $\alpha_s$  is determined by factors such as link length, bending angles between adjacent links, and the ratio  $c_{i,t}/c_{i,n}$  where the ratio also gives a lower bound for  $\alpha_s$ . The winding angle  $\alpha_s$  is found from

$$\alpha_s(s) = \alpha \cos\left(\frac{\pi}{2l}s\right), \quad (13)$$

Table I. Overview of gaits.

| Gait                         | With passive wheels                 | Without wheels         |
|------------------------------|-------------------------------------|------------------------|
| Concertina                   |                                     | [16] <sup>a</sup>      |
| Lateral undulation           | [4, 14, 15, 17, 18, 47, 48, 71, 72] | [7, 19–21, 29, 57, 73] |
| Sidewinding                  |                                     | [26, 29]               |
| Inchworm/Caterpillar         |                                     | [17, 22, 28, 74–76]    |
| Climbing                     |                                     | [77, 78]               |
| Lateral rolling <sup>b</sup> | [71, 79, 80]                        | [17, 81, 82]           |

<sup>a</sup>Utilizes friction from solenoids that are lifted and lowered.

<sup>b</sup>Gait not dependent on wheels for locomotion.

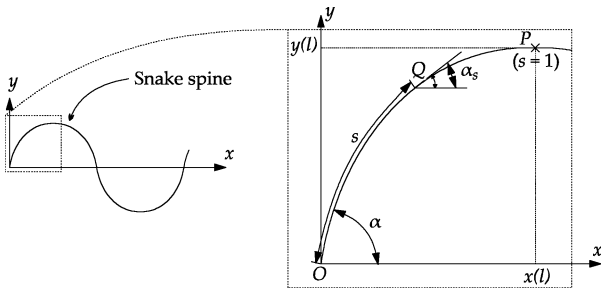


Fig. 5. The serpenoid curve.<sup>3</sup> By permission of Oxford University Press.

where  $\alpha = \alpha_s(0, l)$ . Except when otherwise specified, the common assumption is  $c_{i,t} < c_{i,n}$  which is necessary to move forward on a flat surface by lateral undulation. However, it should be mentioned that a snake robot will instead move slowly *backward* for  $c_{i,t} = c_{i,n}$ .<sup>83</sup>

An alternative to the serpenoid curve has been proposed by Ma<sup>7</sup> and is called the serpentine curve. Ma<sup>7</sup> has shown that a snake robot following this curve has a higher locomotive efficiency. The locomotive efficiency is defined for a snake robot that does not slip as the ratio between the forces that act along the snake robot and the forces that act perpendicular to the body.<sup>7</sup>

**4.1.2. Lateral undulation for snake robots.** The serpenoid curve cannot be exactly reproduced by a snake robot due to its discrete morphology. However, an approximation to the serpenoid curve can be recreated by a snake robot by setting the joint reference angle  $\phi_{i,d}$  for joints  $i = 1, \dots, n - 1$  as

$$\phi_{i,d} = A \sin(\omega t + (i - 1)\beta) + \gamma, \quad (14)$$

where  $A$  is the maximum amplitude of oscillation,  $\beta$  is the phase shift between adjacent links,  $\gamma$  determines the orientation of the snake robot, and  $\omega$  is the angular frequency of oscillation. The parameters  $\beta$  and  $\omega$  determine the speed of the serpentine wave that propagates down the body of the snake robot (see e.g. the papers by Ye *et al.*<sup>72</sup> and Saito *et al.*).<sup>19</sup> The use of  $\gamma$  to change the heading of the snake is discussed by Ye *et al.*<sup>72</sup> and two alternative turning motions are also presented.

Sideways slip should be kept as low as possible when moving by lateral undulation. This is because such slip does not contribute to forward motion. For wheel-less snake robots, sideways slip can be reduced by changing the motion pattern parameters in Eq. (14) according to the ratio  $c_{i,t}/c_{i,n}$ . An example on how to do this has been presented by Saito *et al.*<sup>19</sup> where the desired relative joint angles are found from Eq. (14) and experimental results are given for a snake robot without wheels. In addition, it is shown how to control the speed and heading of the snake robot to desired values by altering  $\omega$  and  $\gamma$  in Eq. (14), respectively.<sup>19</sup>

Another way of reducing sideways slip is to mechanically alter the snake robot by adding passive caster wheels to the belly. For the snake robot ACM III (in Fig. 1) used as an example by Ostrowski and Burdick,<sup>14</sup> the angle between adjoining links and the angle between the wheel axles and the links are set  $90^\circ$  out of phase to move forward while avoiding wheel slip. A model that is similar to the ACM III,

but with fixed wheel axles, is employed by Prautsch and Mita.<sup>47</sup> This work proposes a Lyapunov-based approach for position control of the head of the snake robot. In addition, it is shown how to minimize the control torques required for serpentine motion. Hence, the low control torques reduce the risk of wheel slip. Date *et al.*<sup>84</sup> introduce an expression for the constraint forces introduced by the wheels and a control approach based on dynamic manipulability is proposed to avoid sideways slip. A control strategy to avoid wheel slip is also presented in a later paper by Date *et al.*<sup>85</sup> The latter approach uses an automatic generation of the joint reference signals based on a velocity reference for the head of the snake robot while keeping a winding shape of the robot. The results given by Date *et al.*<sup>85</sup> are extensions of the methods presented by Prautsch and Mita<sup>47</sup> where the snake robot tended to a singular (straight) posture when the number of links was increased.<sup>84</sup> Results on the controllability of snake robots are given by Kelly *et al.*<sup>32</sup> and Ostrowski and Burdick.<sup>86</sup>

McIsaac and Ostrowski<sup>21,58,87</sup> have derived and implemented closed-loop heading control based on image-based position feedback for an underwater snake robot, and a controller for stopping the underwater snake robot during forwards and circular motion is presented. The motion pattern for underwater locomotion is similar to lateral undulation.

Ma *et al.*<sup>15,88</sup> study lateral undulation on an inclined surface. It is found that in order for the snake robot to be able to move up the plane, the upper limit for the initial winding angle  $\alpha$  decreases and the lower limit increases for increasing inclination angles of the plane.

While most of the approaches to locomotion presented above rely on the tangential/normal friction property, others have explored alternative ways to locomotion where either the friction model is isotropic or a purely kinematic model is used. Biological snakes exploit obstacles such as rocks or contours on the ground to aid locomotion during lateral undulation as mentioned in Section 2.3.1. This form of locomotion has also been investigated for snake robots.<sup>3,62,89-91</sup> The pioneering work on such locomotion was presented by Hirose and Umetani<sup>89</sup> where it is suggested how to utilize walls and large cylinders to generate propulsive forces for a wheeled snake robot (see also Hirose's book).<sup>3</sup> Two decades later, an approach to locomotion was presented where the snake robot is allowed to come in contact with the obstacles<sup>16</sup> and it is discussed how the snake robot can continue to be mobile while in contact with an obstacle. The links of the snake robot presented have ball casters to slide on and solenoids to push into the ground surface to increase friction when needed. With this snake robot, the change in number of degrees of freedom of each link while in contact with the obstacles is investigated and the obstacles are used as constraints so that the snake robot is able to slide along them. More recently, Bayraktaroglu and Blazevic<sup>90</sup> have presented a snake robot without wheels that employs push-points, such as pegs, to create the total propulsive force during a form of lateral undulation. Here, the ratio between lateral and longitudinal friction is disregarded, which makes it possible to build and develop motion patterns for snake robots without the friction property  $c_{i,t} < c_{i,n}$ , and hence without wheels. The joints are not bent to push against the pegs; instead, the snake robot<sup>90</sup> has linear actuators on each

side of the links that push out from the link. This work has been extended by Bayraktaroglu *et al.*<sup>91</sup> where the linear actuators are no longer necessary. Instead, the wheel-less snake robot localizes push-points with on/off switch sensors along the sides of its body. The snake robot then calculates a spline between two adjacent push-points and the joint angles are controlled so that its body is fitted to the spline and thus uses the push-points to be able to move forward. It is assumed that there is always a push-point available within reasonable proximity of the head of the snake robot. Experimental results are presented for this approach. The serpenoid curve was not employed directly in the paper by Bayraktaroglu<sup>90,91</sup> due to the change of shape according to the placement of the push-points, however, the similarities to the shape of a biological snake moving by lateral undulation while using contours on the ground to push against are apparent.

**4.1.3. Alternative Approaches to Locomotion.** Planar locomotions for a two-link, three-link, and multi-link system with 1-DOF revolute joints are shown by Chernousko.<sup>54,55</sup> Dry friction forces between the links and the ground is assumed. A combination of fast and slow movements of the joints is used to move the two- and three-link system to any point in the plane. With very small velocities and accelerations, the multi-link system was able to move by propagating a single wave (consisting of three to four links) at a time forward along the snake robot body. Subsequently, locomotion is obtained as long as the moving part of the snake robot is not subjected to a friction force larger than what the non-moving part is able to counteract by lying still. This principle is similar the concertina locomotion (see Section 2.3.2) except that the snake robot does not anchor its body by pushing against something other than the flat ground surface—for example the walls of a narrow passage.

#### 4.2. 3D snake robot locomotion

For snake robots with 2-DOF revolute joints and capable of 3D motion, a second reference signal is needed to control the vertical wave. The joint reference signal can be written as

$$\phi_{v_i,d} = A_v \sin(\omega_v t + (i - 1)\beta_v + \beta_0), \quad (15)$$

where  $\phi_{v_i,d}$  is the relative angle of joint  $i$  that controls the lift of the adjacent links.<sup>29</sup> The phase difference between the horizontal and vertical waves is given by  $\beta_0$  and the remaining parameters  $A_v$ ,  $\omega_v$ , and  $\beta_v$  have the same interpretation as the parameters in Eq. (14). The direction of locomotion when using lateral undulation ( $A_v = 0$ ) is controlled by  $\gamma$ .

Sinus-lifting is also implemented for snake robots.<sup>50,71,92</sup> A 2D model incorporating a ground contact force which is a function of the curvature of the snake body is used by Ma *et al.*<sup>50</sup> It is shown that the snake robot moves forward faster by sinus-lifting, than by lateral undulation. In addition, sinus-lifting is a way of reducing the risk of side slip of the wheels. A control method for determining which links to lift based on a kinematic model has been proposed by Ohmameuda and Ma.<sup>93</sup> A wheeled snake robot able to move in 3D is presented by Ma *et al.*<sup>48</sup> and it is shown that for the robot to be controllable and observable, the number of wheels  $m$  must satisfy the condition  $4 \leq m \leq n - 2$ , where  $m$  is the number

of pairs of wheels touching the ground simultaneously and  $n$  is the number of DOF of the snake robot. Sinus-lifting, like lateral undulation, is dependent on an anisotropic friction property ( $c_{t,i} < c_{n,i}$ ) for efficient locomotion. However, there are also motion patterns for moving with isotropic friction. These motion patterns will be elaborated in the following three paragraphs.

Sidewinding was implemented with  $c_{t,i} = c_{n,i}$  by Liljebäck<sup>53</sup> using (14) and (15) to find the desired joint angles, and it was found that both  $\gamma$  and  $\beta_0$  control the direction of locomotion. A slightly different approach to sidewinding locomotion is developed by Burdick *et al.*<sup>26</sup> for 3D motion on a flat surface. In this latter work, the snake robot lays its stationary parts flat on the ground while the moving parts are curved above the ground (see Section 2.3.3 for how sidewinding is performed). This results in a more natural gait compared to a sinus-like curve for the shape of a snake robot that is obtained by employing (14) and (15) to find the desired joint angles. The use of such a sinus-like curve results in that the snake robot only touches the ground surface at single points when the joint angles are accurately controlled, thus decreasing stability. Sidewinding has also been performed where an expression for the shape or joint angles is not found in advance. One such approach is the use of genetic programming to develop a form of sidewinding.<sup>94</sup> Hence, the snake robot determines how to move its joints based on some desired criteria. Moreover, simulation results are given where the snake robot manages to move sideways despite several joints being damaged.

Inchworm-like and caterpillar-like motion patterns are shown with<sup>22,75</sup> and without<sup>22,28,74,76</sup> extensible joints (see Fig. 6(b) for the latter case). These gaits have mostly been modeled by only considering the kinematics (and not the dynamics) of the snake robot. The model is nevertheless valid since it is assumed that the snake robot is moving slowly. While some<sup>22,28</sup> rely on slow speeds to avoid slipping, water can also be pumped between the links to add weight to the parts that are not moving.<sup>74</sup> This way, the ground contact force and hence the friction on the moving parts is reduced.

Various kinds of rolling motion have also been proposed. These motion patterns are not directly similar to movement of biological snakes. Lateral rolling is a sub-group of these motion patterns. One way of implementing lateral rolling consists of moving all the joints in phase while keeping the snake robot in a U-shape on the ground<sup>81</sup> as in Fig. 6(a). Experimental results for this gait are given by e.g. Hirose and Mori.<sup>71,92</sup> U-shaped lateral rolling is mainly performed with all links in contact with the ground surface. However, 2-DOF (cardan) joints are still needed so the snake robot has to be capable of 3D motion (the robot can also be equipped with alternating perpendicular 1-DOF joints instead of 2-DOF joints). Other forms of lateral rolling are described by Chen *et al.*<sup>82</sup> Another way of moving proposed in the same paper is called the “smoke ring”<sup>81</sup> as depicted in Fig. 6(e). The snake robot then shapes its body into a ring and subsequently curls around a vertical or horizontal pipe-like structure in order to “roll” along the pipe. The snake robot can also move like a wheel as shown in Fig. 6(c) and Yim<sup>75</sup> shows how to employ this gait in a turning motion. However, it is challenging to keep the snake robot from falling over

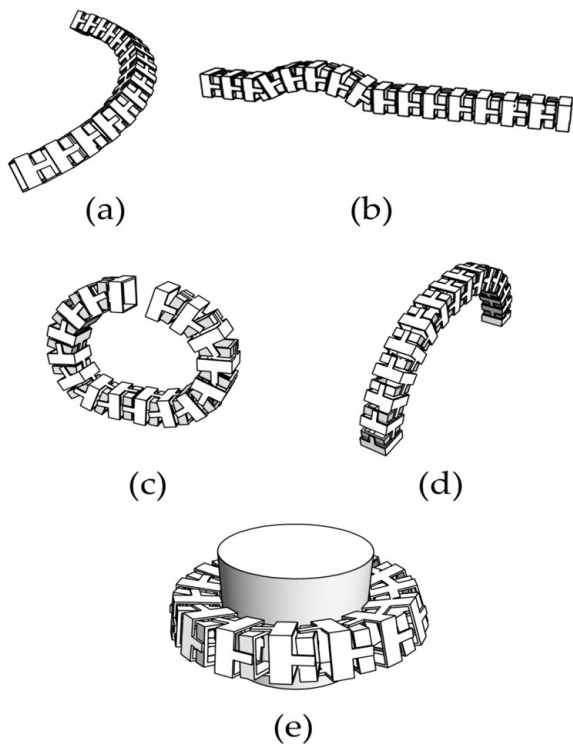


Fig. 6. Various motion patterns implemented on snake robots: (a) U-shaped lateral rolling (moving towards the right), (b) traveling wave/caterpillar locomotion (moving the same way as the traveling wave, i.e. left or right), (c) the wheel (moving right or left), (d) bridge mode (moving right or left), and (e) “smoke ring” (moving upwards or downwards).

while moving. A form of this wheel-like motion strategy is employed by Yim *et al.*<sup>75</sup> to climb stairs with a snake robot. The shape of the snake robot is described analytically for several motion patterns based on rolling (or “twisting”) by Ye *et al.*<sup>95</sup> In the latter paper, sinus-lifting and other common serpentine motion patterns have been combined with a twisting motion. Moreover, several of these motion patterns are tested by experiments and all tests show mainly a sideways motion of the snake robot. Erkmén *et al.*<sup>96</sup> have also elaborated on the twisting mode of locomotion where an approach on how to make the snake robot walk using its two ends as feet is described. This form of locomotion is called “bridge mode” and is illustrated in Fig. 6(d). In addition, a genetic algorithm is presented that handles how to move the snake robot from lying flat on the ground to standing on its two ends without losing structural stability. Descriptive figures and explanations of several of the gaits mentioned above, in addition to other motion patterns, are found given by Ohno and Hirose,<sup>17</sup> Dowling,<sup>81</sup> and Mori and Hirose.<sup>71</sup> Moreover, movies of various snake robots during locomotion can be found on the web.<sup>97,98</sup>

A snake robot, called the ACM-R5, with fins with wheels on its link and thus capable of both swimming and land-based locomotion is presented by Yamada *et al.*<sup>79</sup> The snake robot moves on land by lateral rolling and lateral undulation. In the water, it can move up and down, swim forwards, and turn. The details of the motion patterns are said to be reported on a later stage.<sup>79</sup>

The snake robot needs to lift its body when for example climbing or moving over high obstacles. However, the joint actuators can only produce a limited torque. Hence, the snake robot links should be lifted in some “intelligent” manner to keep the necessary joint torques as low as possible. To this end, Nilsson<sup>77,78</sup> has developed an algorithm for lifting several links with limited joint torque. In addition, the snake robot may utilize poles or other objects for climbing and a variant of the “smoke ring” in Fig. 6(e) has been proposed by Nilsson.<sup>99</sup>

## 5. Discussion and Future Research Topics

Research on snake robots has increased over the past 10–15 years, but many challenges concerning modeling and control of snake robots still remain before these mechanisms are able to locomote intelligently through unknown terrain. We have shown in this paper that various approaches to mathematical modeling of snake robots have been presented. Some focus purely on the kinematic aspects of locomotion<sup>14,22,36,86</sup> while others also include the dynamics.<sup>4,15,19,47,51,57</sup> The use of a purely kinematic model simplifies both the model and the analysis of locomotion, and factors that contribute to locomotion have been highlighted.<sup>14</sup> Passive wheels help defend the no-slip assumption of some kinematic models, but it may be difficult to control the joint torques such that the wheels do not slip.<sup>4,15</sup> A kinematic approach to locomotion without wheels is justified by assuming low velocities and sometimes also certain friction properties (such as low friction while gliding forwards, but high friction when pushed backwards).<sup>22</sup>

There are mainly two reasons to model a system mathematically. One is that the model can be used to analytically investigate how to control the system. The other reason is to simulate the behavior of the system, for example for testing motion patterns. Mathematical models that include the dynamics of motion yield a more accurate description of the behavior of the system which is advantageous with respect to simulation, but the models may get very large and unwieldy. Thus, the simplicity of an analytical analysis suffers. In 2D models, certain properties of the system help to simplify the model,<sup>21</sup> but not all of these properties persist in 3D models. In the papers presented, most models are 2D, but moving in a shattered building, for example, is an inherently 3D experience. 3D models have been presented<sup>22,26,48</sup> where some results on controllability and observability are also presented.<sup>48</sup> However, the dynamics has not been considered. During recent years, 3D dynamic models based on the Newton–Euler equations have been presented.<sup>29,50,51</sup> Ma *et al.*<sup>50</sup> have derived mathematical expressions for the joint torques and head configuration, but for the gait analysis, the model has been simplified to planar movement with a varying ground contact force which affects the friction forces on each link. Hence, there are still numerous challenges in the analytical investigation of the dynamics of 3D locomotion.

Regardless of the downsides of dynamic modeling, the dynamics needs to be considered in the cases where slow locomotion is unacceptable or when wheels cannot be employed due to the nature of the surface traveled on. In such cases, friction and impacts need to be considered and

utilized to aid locomotion. Two models have been found in the literature that describe the normal contact forces between a snake robot and its environment. The first approach models the contact force using a linear spring-damper model.<sup>29</sup> This is a very intuitive approach and easy to implement. However, the large spring coefficient needed to resemble a hard ground surface results in a stiff mathematical model which requires a small step length to avoid instability in the numerical integration. The second approach models impacts between rigid bodies as instantaneous using methods from nonsmooth dynamics.<sup>51,52,62</sup> Thus, model stiffness is less of a problem. However, there is a certain threshold in order to get familiar with force laws written in the framework of convex analysis and nonsmooth dynamics.

Friction forces are modeled either as viscous friction or based on Coulomb's law of dry friction, where the latter includes a stick phase which is essential for some gaits.<sup>55</sup> The directional friction property between the belly of the snake and the ground, most often implemented on snake robots, cannot always be realized for travel due to varying ground conditions. Snakes utilize contours on the ground to push against for faster and more efficient locomotion. This form of locomotion by pushing against objects has been investigated for snake robots,<sup>3,91,100</sup> and experiments with a wheel-less snake robot that moves forwards by pushing against pegs have been presented.<sup>62,91</sup>

By going through the published literature, we see that there are several aspects of snake robot locomotion. The main concern is to find some kind of (often repetitive) reference for the joint angles such that the snake robot moves in some direction. A large variety of pre-programmed reference signals have been proposed resulting in different motion patterns. The pre-programmed motion patterns can be improved and extended by incorporating feedback from external measurements of, for example, velocity, heading, and/or position of the snake robot<sup>19,87,101</sup> into the generation of the joint reference angles. Others focus on finding optimal pre-programmed motion patterns with respect to energy consumption and distance traveled.<sup>7,50</sup> Some snake robots are equipped with sensors and the motion pattern is then generated based on continuously updated measurements from the sensors.<sup>6,91,102</sup> The sensors may be used to detect contours on the ground that can be pushed against for faster locomotion. In addition, sensors can be used for real-time generation of maps of the environment surrounding the snake robot in order to find a feasible path.<sup>103,104</sup> A combination of all the above capabilities are needed to be able to operate for a sufficiently long time during, for example, a search or maintenance mission.

Based on the above discussion, the following future research topics are proposed: (1) Find ways to better use pegs or other obstacles to improve locomotion speed and efficiency, (2) investigate closed-loop heading and velocity control based on on-board sensors, and (3) develop a mathematical framework to help develop and prove efficiency of general motion patterns.

## 6. Conclusion

It is not clear which modeling approach is "the best" for a certain situation since all strategies have advantages and

disadvantages and various criteria need to be considered. These are for example: What theoretical background does a person who is going to do the modeling have? Is it sufficient to only consider the kinematics or must the dynamics also be included? What is the purpose of making the model—only simulations or analytical considerations regarding snake robot control and locomotion? These questions should be carefully considered before choosing a specific approach. The respective sections in this paper dealing with the various approaches give the reader an overview of the different methods and also an idea of what background knowledge it is necessary to possess in order to easily apply the respective methods. We will now summarize various modeling approaches with respect to the issues described above concerning which model to choose.

First of all, if only a description of what a planar snake robot looks like given a specified set of joint angles is needed, then a simple description of the kinematics like the one given by Ma<sup>18</sup> suffices. This method is based on direct calculation of the kinematics based on joint angles and link lengths. However, if the same relationship is to be found for a 3D snake robot, then such an approach may prove cumbersome. Instead, the D-H convention<sup>29,105</sup> might be more convenient to apply. The D-H convention provides a systematic and general method for describing the kinematics of a robot based on a recursive expression. Hence, relative rotations between adjacent links need only to be handled 1-DOF at the time instead of always calculating the position and orientation of each link in 3D space directly. Both of the above methods are relatively easy to implement. If the goal is to study various shapes of a snake robot and then transform these shapes into corresponding joint angles, then the method of backbone curves proposed by Chirikjian *et al.*<sup>12</sup> may be more appropriate. However, the effort needed to get a clear understanding of the relevant theory regarding backbone curves may be considerable and this needs to be taken into account when choosing an appropriate modeling technique. Nevertheless, the backbone curve allows researchers to focus more on the actual *shape* of a snake robot, rather than its individual joint angles which are the starting point for doing modeling with the previously mentioned methods.

The dynamics of motion needs to be included when elements such as friction and contact forces are important. The 2D model probably easiest to implement is given by Saito *et al.*<sup>106</sup> and this model can also be employed to develop model-based control algorithms for speed and heading of a snake robot. This approach is based on the standard Newton–Euler formulation where each link is initially treated independently by describing their linear and angular motion. Then the links are connected to each other by joints which constitute bilateral constraint forces. The Lagrangian formulation differs from the Newton–Euler formulation in that the snake robot model is treated as a whole from the beginning and the modeling is performed using a Lagrangian function which includes the energy of the system. The Lagrangian formulation and the Newton–Euler formulation are similar for rigid body dynamics in that the final answers are the same. However, one could argue that the Newton–Euler formulation is the most suitable method for finding the torques that need to be applied to

get a desired motion, while the Lagrangian formulation is superior for describing the time evolution of the generalized coordinates of the system.<sup>107</sup> For someone familiar with the Lagrangian formulation and geometric mechanics, the 2D model presented by McIsaac and Ostrowski<sup>21</sup> could prove advantageous since a framework for control of the momentum of a snake robot is now available. However, it may be demanding and time consuming for someone who is not acquainted with the basic principles of geometric mechanics to thoroughly understand these methods. This also applies for the nonsmooth 2D model presented by Transeth *et al.*<sup>108</sup> where the Newton–Euler formulation is used together with set-valued force laws. The advantages with this latter approach are true stick–slip transitions and a relatively easy method for modeling contact with obstacles.

Moving on to 3D models of the dynamics of snake robot motion, we have fewer models to choose from. Liljebäck *et al.*<sup>29</sup> have employed standard techniques for modeling robot manipulators in order to develop a 3D snake robot model, and someone accustomed with these general methods would find this approach easy. Another benefit of employing these techniques is that many methods for accurately controlling robot manipulators now become available for snake robots.<sup>109</sup> However, a choice of minimal coordinates and a compliant contact force model renders the resulting set of equations of motion stiff and cumbersome to solve numerically. This is solved in parts by introducing nonminimal coordinates for a nonsmooth 3D model<sup>110</sup> where contact forces are modeled in a rigid-body setting and velocities are allowed to change instantaneously. This model is suited for simulation, but not for analytical considerations. Moreover, getting familiar with the framework of nonsmooth dynamics requires some work. The above summary shows that many aspects need to be considered when choosing an appropriate modeling strategy. We hope that this paper may serve as a guide in order to make this choice more easy.

A snake robot has limited payload capability, poor power efficiency and a high number of DOF. Nevertheless, the snake robot has the potential of great terrainability and the capability of inspecting narrow places. It can also be made very robust to dirt and dust by covering the robot completely with a shell. These properties make the research on snake robots worthwhile. It is hoped that this survey will help promote further research on the fascinating topic of snake robots through the overview given on modeling and locomotion.

## References

- G. Miller, "Snake Robots for Search and Rescue," *In: Neurotechnology for Biomimetic Robots* (MIT Press, Cambridge, MA, USA, 2002) pp. 271–284.
- J. Gray, "The mechanism of locomotion in snakes," *J. Exp. Biol.*, **23**(2), 101–120 (1946).
- S. Hirose, *Biologically Inspired Robots: Snake-Like Locomotors and Manipulators*. (Oxford University Press, Oxford, 1993).
- P. Wiriyacharoensunthorn and S. Laowattana, "Analysis and Design of a Multi-Link Mobile Robot (Serpentine)," *Proceedings of the IEEE International Conference on Industrial Technology*, Bangkok, Thailand, Vol. 2 (Dec. 2002) pp. 694–699.
- M. Lewis and D. Zehnpfennig, "R7: A Snake-Like Robot for 3-D Visual Inspection," *Proceedings of IEEE/RSJ International Conference on Intelligent Robots and Systems*, Munich Germany, Vol. 2 (Sept. 1994) pp. 1310–1317.
- R. Worst and R. Linnemann, "Construction and Operation of a Snake-Like Robot," *Proceedings of IEEE International Joint Symposium on Intelligence and Systems*, Rockville, MD (Nov. 1996) pp. 164–169.
- S. Ma, "Analysis of Snake Movement Forms for Realization of Snake-Like Robots," *Proceedings of IEEE International Conference on Robotics and Automation*, Detroit, MI, Vol. 4 (May 1999) pp. 3007–3013.
- S. Ma, H. Araya, and L. Li, "Development of a Creeping Snake-Robot," *Proceedings of IEEE International Symposium on Computational Intelligence in Robotics and Automation*, Banff, Alberta, Canada (Jul.–Aug. 2001) pp. 77–82.
- Y. Lu, S. Ma, B. Li and L. Chen, "Ground Condition Sensing of a Snake-Like Robot," *Proceedings of IEEE International Conference on Robotics, Intelligent Systems and Signal Processing*, Changsha, Hunan, China, Vol. 2 (Oct. 2003) pp. 1075–1080.
- L. Xinyu and F. Matsuno, "Control of Snake-Like Robot Based on Kinematic Model with Image Sensor," *Proceedings IEEE International Conference on Robotics, Intelligent Systems and Signal Processing*, Changsha, Hunan, China, Vol. 1 (Oct. 2003) pp. 347–352.
- T. Kamegawa, T. Yarnasaki, H. Igarashi and F. Matsuno, "Development of the Snake-Like Rescue Robot 'Kohga'," *Proceedings of IEEE International Conference on Robotics and Automation*, Barcelona, Spain, Vol. 5 (Apr. 2004) pp. 5081–5086.
- G. Chirikjian and J. Burdick, "A modal approach to hyper-redundant manipulator kinematics," *IEEE Trans. Robot. Autom.* **10**(3), 343–354 (Jun. 1994).
- P. Krishnaprasad and D. Tsakiris, "G-snakes: Nonholonomic Kinematic Chains on Lie Groups," *Proceedings of 33rd IEEE Conference on Decision and Control*, Lake Buena Vista, FL, Vol. 3 (Dec. 1994) pp. 2955–2960.
- J. Ostrowski and J. Burdick, "Gait Kinematics for a Serpentine Robot," *Proceedings of IEEE International Conference on Robotics and Automation*, Minneapolis, Minnesota, USA, Vol. 2 (Apr. 1996) pp. 1294–1299.
- S. Ma, N. Tadokoro, B. Li and K. Inoue, "Analysis of Creeping Locomotion of a Snake Robot on a Slope," *Proceedings of IEEE International Conference on Robotics and Automation*, Taipei, Taiwan (Sep. 2003) pp. 2073–2078.
- Y. Shan and Y. Koren, "Design and motion planning of a mechanical snake," *IEEE Trans. Syst. Man Cyb.* **23**(4), 1091–1100 (Jul.–Aug. 1993).
- H. Ohno and S. Hirose, "Design of Slim Slime Robot and Its Gait of Locomotion," *Proceedings of IEEE/RSJ International Conference on Intelligent Robots and Systems*, Wailea, Hawaii, Vol. 2 (Nov. 2001) pp. 707–715.
- S. Ma, "Analysis of creeping locomotion of a snake-like robot," *Adv. Rob.* **15**(2), 205–224 (2001).
- M. Saito, M. Fukaya and T. Iwasaki, "Serpentine locomotion with robotic snakes," *IEEE Contr. Syst. Mag.* **22**(1), 64–81 (Feb. 2002).
- I. Grabec, "Control of a Creeping Snake-Like Robot," *Proceedings of 7th International Workshop on Advanced Motion Control*, Maribor, Slovenia (Jul. 2002) pp. 526–513.
- K. McIsaac and J. Ostrowski, "Motion planning for anguilliform locomotion," *IEEE Trans. Robot. Autom.* **19**(4), 637–625 (Aug. 2003).
- G. Chirikjian and J. Burdick, "The kinematics of hyper-redundant robot locomotion," *IEEE Trans. Robot. Autom.* **11**(6), 781–793, (Dec. 1995).
- C. Mattison, *The Encyclopaedia of Snakes* (Cassell Paperbacks, London, 2002).
- R. Bauchot, *Snakes: A Natural History*, New York, USA (Sterling Publishing Company, 1994).

25. K. J. Dowling, 'Limbless Locomotion. Learning to Crawl with a Snake Robot *Ph.D. Dissertation* (Carnegie Mellon University, Dec. 1997).
26. J. Burdick, J. Radford and G. Chirikjian, "A 'Sidewinding' Locomotion Gait for Hyper-Redundant Robots," *Proceedings of IEEE International Conference on Robotics and Automation*, Atlanta, GA, USA (May 1993) pp. 101–106.
27. R. M. Murray, Z. Li and S. S. Sastry, *A Mathematical Introduction to Robotic Manipulation*, 1st ed. (CRC Press, Florida, USA, 1994).
28. G. Poi, C. Scarabeo and B. Allotta, "Traveling Wave Locomotion Hyper-Redundant Mobile Robot," *Proceedings of IEEE International Conference on Robotics and Automation*, Lueven, Belgium, Vol. 1 (May 1998) pp. 418–423.
29. P. Liljebäck, Ø. Stavadahl and K. Y. Pettersen, "Modular Pneumatic Snake Robot: 3D Modelling, Implementation and Control," *Proceedings of 16th IFAC World Congress*, Prague, Czech Republic (Jul. 2005).
30. I. Kolmanovsky and N. McClamroch, "Developments in nonholonomic control problems," *IEEE Contr. Syst. Mag.* **15**(6), 20–36, (Dec. 1995).
31. A. M. Bloch, J. Baillieul, P. Crouch and J. Marsden, *Nonholonomic Mechanics and Control*, New York, USA (Springer-Verlag, 2003).
32. S. Kelly and R. M. Murray, "Geometric phases and robotic locomotion," *J. Rob. Syst.* **12**(6), 417–431 (1995).
33. G. Chirikjian and J. Burdick, "Kinematics of Hyper-Redundant Robot Locomotion with Applications to Grasping," *Proceedings of IEEE International Conference on Robotics and Automation*, Sacramento, CA, USA (Apr. 1991) pp. 720–725.
34. G. S. Chirikjian, Theory and Applications of Hyper-Redundant Robotic Manipulators *Ph.D. Dissertation* (California Institute of Technology, Pasadena, California, 1992).
35. G. S. Chirikjian, "Design and analysis of some nonanthropomorphic, biologically inspired robots: An overview," *J. Rob. Syst.* **18**(12), 701–713 (Dec. 2001).
36. H. Yamada and S. Hirose, "Study on the 3d Shape of Active Cord Mechanism," *Proceedings of IEEE International Conference on Robotics and Automation*, Orlando, FL, USA (2006) pp. 2890–2895.
37. M. P. Do Carmo, *Differential Geometry of Curves and Surfaces* (Prentice-Hall, Englewood Cliffs, New Jersey, 1976).
38. Y. Wang and G. Chirikjian, "Workspace generation of hyper-redundant manipulators as a diffusion process on  $se(n)$ ," *IEEE Trans. Rob. Automat.* **20**(3), 399–408 (Jun. 2004).
39. G. Robinson and J. B. C. Davies, "Continuum Robots – A State of the Art," *Proceedings of IEEE International Conference on Robotics and Automation*, Detroit, MI, USA, Vol. 4 (May 1999) pp. 2849–2854.
40. B. Jones and I. Walker, "Kinematics for multisection continuum robots," *IEEE Transactions on Robotics*, **22**(1), 43–55 (Feb. 2006).
41. M. Hannan and I. Walker, "Kinematics and the implementation of an elephant's trunk manipulator and other continuum style robots," *J. Rob. Syst.* **20**(2), 45–63 (Feb. 2003).
42. I. Gravagne and I. Walker, "Kinematic Transformations for Remotely-Actuated Planar Continuum Robots," *Proceedings of IEEE International Conference on Robotics and Automation*, San Francisco, CA, USA, Vol. 1 (2000) pp. 19–26.
43. I. Gravagne and I. Walker, "On the Kinematics of Remotely-Actuated Continuum Robots," *Proceedings of IEEE International Conference on Robotics and Automation*, San Francisco, CA, USA, Vol. 3 (2000) pp. 2544–2550.
44. H. Mochiyama and H. Kobayashi, "The Shape Jacobian of a Manipulator with Hyper Degrees of Freedom," *Proceedings of IEEE International Conference on Robotics and Automation*, Detroit, MI, USA, Vol. 4 (1999) pp. 2837–2842.
45. H. Mochiyama, E. Shimemura and H. Kobayashi, "Direct Kinematics of Manipulators with Hyper Degrees of Freedom and Frenet–Serret Formula," *Proceedings of IEEE International Conference on Robotics and Automation*, Lueven, Belgium, Vol. 2 (May 1998) pp. 1653–1658.
46. H. Mochiyama, E. Shimemura and H. Kobayashi, "Shape Correspondence Between a Spatial Curve and a Manipulator with Hyper Degrees of Freedom," *Proceedings of IEEE/RSJ International Conference on Intelligent Robots and Systems*, Victoria, Canada, Vol. 1 (1998) pp. 161–166.
47. P. Prautsch and T. Mita, "Control and Analysis of the Gait of Snake Robots," *Proceedings of IEEE International Conference on Control Applications*, Kohala Coast, HI (1999) pp. 502–507.
48. S. Ma, Y. Ohmameuda, K. Inoue and B. Li, "Control of a 3-Dimensional Snake-Like Robot," *Proceedings of IEEE International Conference on Robotics and Automation*, Taipei, Taiwan, Vol. 2 (Sep. 2003) pp. 2067 – 2072.
49. O. Egeland and J. T. Gravdahl, *Modeling and Simulation for Automatic Control* (Marine Cybernetics, Trondheim, Norway, 2002).
50. S. Ma, Y. Ohmameuda and K. Inoue, "Dynamic Analysis of 3-Dimensional Snake Robots," *Proceedings of IEEE/RSJ International Conference on Intelligent Robots and Systems*, Sendai, Japan (2004) pp. 767–772.
51. A. A. Transeth, R. I. Leine, Ch. Glocker and K. Y. Pettersen, "Non-Smooth 3D Modeling of a Snake Robot with Frictional Unilateral Constraints," *Proceedings of IEEE International Conference on Robotics and Biomimetics*, Kunming, China (Dec. 2006) pp. 1181–1188.
52. A. A. Transeth, R. I. Leine, Ch. Glocker and K. Y. Pettersen, "Non-Smooth 3D Modeling of a Snake Robot with External Obstacles," *Proceedings of IEEE International Conference on Robotics and Biomimetics*, Kunming, China (Dec. 2006) pp. 1189–1196.
53. P. Liljebäck, Modular Snake-Robot: Modeling, Implementation and Control of a Modular and Pressure Based Snake-Robot *Master's Thesis* (Norwegian University of Technology and Science, Trondheim, Norway, 2004).
54. F. Chernousko, "Snake-Like Motions of Multibody Systems Over a Rough Plane," *Proceedings of Second International Conference on Control of Oscillations and Chaos*, Saint-Petersburg, Russia (Jul. 2000) pp. 321–326.
55. F. Chernousko, "Modelling of snake-like locomotion," *Appl. Math. Comput.* **164**(2), 415–434 (May 2005).
56. S. Ma, W. Li and Y. Wang, "A Simulator to Analyze Creeping Locomotion of a Snake-Like Robot," *Proceedings of IEEE International Conference on Robotics and Automation*, Seoul, Korea, Vol. 4 (2001) pp. 3656–3661.
57. K. McIsaac and J. Ostrowski, "A Geometric Approach to Anguilliform Locomotion: Modelling of an Underwater Eel Robot," *Proceedings of IEEE International Conference on Robotics and Automation*, Detroit, MI, USA, Vol. 4 (May 1999) pp. 2843–2848.
58. K. McIsaac and J. Ostrowski, "Motion Planning for Dynamic Eel-Like Robots," *Proceedings of IEEE International Conference on Robotics and Automation*, San Francisco, CA, USA, Vol. 2 (2000) pp. 1695–1700.
59. J. Ayers, C. Wilbur and C. Olcott, "Lamprey Robots," *Proceedings of International Symposium on Aqua Biomechanisms*, Honolulu, HI, USA (2000) pp. 1–6.
60. A. Bloch, P. Krishnaprasad, J. Marsden and R. Murray, "Nonholonomic Mechanical Systems with Symmetry," Technical Report (California Institute of Technology, 1995).
61. F. Boyer, M. Porez and W. Khalil, "Macro-continuous computed torque algorithm for a three-dimensional eel-like robot," *IEEE Trans. Robot.* **22**(4), 763–775 (2006).
62. A. A. Transeth, P. Liljebäck and K. Y. Pettersen, "Snake Robot Obstacle Aided Locomotion: An Experimental Validation of a

- Non-Smooth Modeling Approach,” *Proceedings of IEEE/RSJ International Conference on Intelligent Robots and Systems*, San Diego, CA (Oct.–Nov. 2007) pp. 2582–2589.
63. G. Chirikjian, “Hyper-redundant manipulator dynamics: A continuum approximation,” *Adv. Rob.* **9**(3), 217–243 (1995).
  64. H. Mochiyama, “Hyper-Flexible Robotic Manipulators,” *IEEE International Symposium on Micro-NanoMechatronics and Human Science*, Nagoya, Japan (Nov. 2005) pp. 41–46.
  65. H. Mochiyama and T. Suzuki, “Kinematics and Dynamics of a Cable-Like Hyper-Flexible Manipulator,” *Proceedings of IEEE International Conference on Robotics and Automation*, Taipei, Taiwan, Vol. 3 (Sep. 2003) pp. 3672–3677.
  66. H. Mochiyama and T. Suzuki, “Dynamics Modelling of a Hyper-Flexible Manipulator,” *Proceedings of the 41st SICE Annual Conference*, Osaka, Japan, Vol. 3 (Aug. 2002) pp. 1505–1510.
  67. I. Gravagne, C. Rahn and I. Walker, “Large deflection dynamics and control for planar continuum robots,” *IEEE/ASME Trans. Mechatron.* **8**(2), 299–307 (Jun. 2003).
  68. J. Wilson, U. Mahajan, S. A. Wainwright and L. Croner, “A continuum model of elephant trunks,” *J. Biomech. Eng.* **113**(1), 79–84 (Feb. 1991).
  69. H. Yamada and S. Hirose, “Development of practical 3-dimensional active cord mechanism ACM-R4,” *J. Rob. Mechatronics* **18**(3), 1–7 (2006).
  70. A. Masayuki, T. Takayama and S. Hirose, “Development of “Souryu-III”: Connected Crawler Vehicle for Inspection Inside Narrow and Winding Spaces,” *Proceedings of IEEE International Conference on Intelligent Robots and Systems*, Sendai, Japan, Vol. 1 (2004), pp. 52–57.
  71. M. Mori and S. Hirose, “Three-Dimensional Serpentine Motion and Lateral Rolling by Active Cord Mechanism ACM-R3,” *Proceedings of IEEE/RSJ International Conference on Intelligent Robots and Systems*, Lausanne, Switzerland (2002) pp. 829–834.
  72. C. Ye, S. Ma, B. Li and Y. Wang, “Turning and Side Motion of Snake-Like Robot,” *Proceedings of IEEE International Conference on Robotics and Automation*, Barcelona, Spain, Vol. 5 (2004) pp. 5075–5080.
  73. Z. Bayraktaroglu, F. Butel, P. Blazevic and V. Pasqui, “A Geometrical Approach to the Trajectory Planning of a Snake-Like Mechanism,” *Proceedings of IEEE/RSJ International Conference on Intelligent Robots and Systems*, Kyongju, Korea (Oct. 1999) pp. 1322–1327.
  74. D. Rincon and J. Sotelo, “Ver-Vite: Dynamic and experimental analysis for inchwormlike biomimetic robots,” *IEEE Robot. Autom. Mag.* **10**(4), 53–57 (Dec. 2003).
  75. M. Yim, “New Locomotion Gaits,” *Proceedings of IEEE International Conference on Robotics and Automation*, San Diego, CA, USA, Vol. 3 (May 1994) pp. 2508–2514.
  76. M. Yim, D. Duff and K. Roufas, “Walk on the wild side,” *IEEE Rob. Automat. Mag.* **9**(4), 49–53 (Dec. 2002).
  77. M. Nilsson, “Snake Robot Free Climbing,” *Proceedings of IEEE International Conference on Robotics and Automation*, Albuquerque, NM, USA, Vol. 4 (Apr. 1997) pp. 3415–3420.
  78. M. Nilsson, “Snake robot – Free climbing,” *IEEE Contr. Syst. Mag.* **18**(1), 21–26 (Feb. 1998).
  79. H. Yamada, S. Chigisaki, M. Mori, K. Takita, K. Ogami and S. Hirose, “Development of Amphibious Snake-Like Robot ACM-R5,” *Proceedings of 36th International Symposium on Robotics*, Tokyo, Japan (Nov.–Dec. 2005).
  80. K. Togawa, M. Mori and S. Hirose, “Study on Three-Dimensional Active Cord Mechanism: Development of ACM-R2,” *Proceedings of IEEE/RSJ International Conference on Intelligent Robots and Systems*, Takamatsu, Japan, Vol. 3 (2000) pp. 2242–2247.
  81. K. Dowling, “Limbless Locomotion: Learning to Crawl,” *Proceedings of IEEE International Conference on Robotics and Automation*, Detroit, MI, USA, Vol. 4 (1999) pp. 3001–3006.
  82. L. Chen, Y. Wang, S. Ma and B. Li, “Studies on Lateral Rolling Locomotion of a Snake Robot,” *Proceedings of IEEE International Conference on Robotics and Automation*, Barcelona, Spain (2004) pp. 5070–5074.
  83. M. Nilsson, “Serpentine Locomotion on Surfaces with Uniform Friction,” *Proceedings of IEEE/RSJ International Conference on Intelligent Robots and Systems*, Sendai, Japan (2004) pp. 1751–1755.
  84. H. Date, Y. Hoshi and M. Sampei, “Locomotion Control of a Snake-Like Robot Based on Dynamic Manipulability,” *Proceedings of IEEE/RSJ International Conference on Intelligent Robots and Systems*, Takamatsu, Japan (2000) pp. 2236–2241.
  85. H. Date, Y. Hoshi, M. Sampei and N. Shigeki, “Locomotion Control of a Snake Robot with Constraint Force Attenuation,” *Proceedings of American Control Conference*, Boston, MA, USA (2001) pp. 113–118.
  86. J. Ostrowski and J. Burdick, “The geometric mechanics of undulatory robotic locomotion,” *Int. J. Robot. Res.* **17**(7), 683–701 (1998).
  87. K. A. McIsaac and J. P. Ostrowski, “A framework for steering dynamic robotic locomotion systems,” *Int. J. Robot. Res.* **22**(2), 83–97 (Feb. 2003).
  88. S. Ma and N. Tadokoro, “Analysis of creeping locomotion of a snake-like robot on a slope,” *Autonom. Rob.* **20**, 15–23 (2006).
  89. S. Hirose and Y. Umetani, “Kinematic Control of Active Cord-Mechanism with Tactile Sensors,” *Proceedings of Second RoManSy Symposium*, Warsaw (1976) pp. 241–252.
  90. Z. Bayraktaroglu and P. Blazevic, “Understanding snakelike locomotion through a novel push-point approach,” *J. Dyn. Syst. – Trans. ASME* **127**(1), 146–152 (Mar. 2005).
  91. Z. Y. Bayraktaroglu, A. Kilicarslan, A. Kuzucu, V. Hugel and P. Blazevic, “Design and Control of Biologically Inspired Wheel-Less Snake-Like Robot,” *Proceedings of IEEE/RAS-EMBS International Conference on Biomedical Robotics and Biomechatronics*, Pisa, Italy (Feb. 2006) pp. 1001–1006.
  92. S. Hirose and M. Mori, “Biologically Inspired Snake-Like Robots,” *Proceedings of IEEE International Conference on Robotics and Biomimetics*, Shenyang, China (Aug. 2004) pp. 1–7.
  93. Y. Ohmameuda and S. Ma, “Control of a 3-Dimensional Snake-Like Robot for Analysis of Sinus-Lifting Motion,” *Proceedings of 41st SICE Annual Conference*, Osaka, Japan, Vol. 3 (2002) pp. 1487–1491.
  94. I. Tanev, T. Ray and A. Buller, “Automated evolutionary design, robustness, and adaptation of sidewinding locomotion of a simulated snake-like robot,” *IEEE Trans. Rob.* **21**(4), 632–645 (Aug. 2005).
  95. C. Ye, S. Ma, B. Li and Y. Wang, “Twist-Related Locomotion of a 3D Snake-Like Robot,” *Proceedings of IEEE International Conference on Robotics and Biomimetics*, Shenyang, China (Aug. 2004) pp. 589–594.
  96. I. Erkmén, A. Erkmén, F. Matsuno, R. Chatterjee and T. Kamegawa, “Snake robots to the rescue!” *IEEE Rob. Automat. Mag.* **9**(3), 17–25 (2002).
  97. H. Choset, “Snake robots at Carnegie Mellon University,” <http://www.snakerobot.com/> (2007), online. Accessed September 29, 2007.
  98. G. Miller, “Dr. Miller’s snake robots,” <http://www.snakerobots.com/> (2007), online. Accessed September 29, 2007.
  99. M. Nilsson, “Ripple and Roll: Slip-Free Snake Robot Locomotion,” *Proceedings of Mechatronical Computer Systems for Perception and Action*, Pisa, Italy (Feb. 1997).
  100. Z. Bayraktaroglu, F. Butel, V. Pasqui and P. Blazevic, “Snake-like locomotion: Integration of geometry and kineto-statics,” *Adv. Rob.* **14**(6), 447–458 (2000).
  101. K. A. McIsaac and J. P. Ostrowski, “Motion Planning for Dynamic Eel-Like Robots,” *Proceedings of IEEE International Conference on Robotics and Automation*, San Francisco, CA, USA, Vol. 2 (Apr. 2000) pp. 1695–1700.

102. K. Ito and Y. Fukumori, "Autonomous Control of a Snake-Like Robot Utilizing Passive Mechanism," *Proceedings of IEEE International Conference on Robotics and Automation*, Orlando, FL, USA (May 2006) pp. 381–386.
103. H. Choset and J. Y. Lee, "Sensor-based construction of a retract-like structure for a planar rod robot," *IEEE Trans. Robot. Autom.* **17**(4), 435–449 (2001).
104. W. Henning, F. Hickman and H. Choset, "Motion Planning for Serpentine Robots," *Proceedings of ASCE Space and Robotics*, Albuquerque, NM, USA (1998).
105. L. Sciavicco and B. Siciliano, *Modelling and Control of Robot Manipulators*, 2nd ed. (McGraw Hill Inc., London, 1999).
106. M. Saito, M. Fukaya and T. Iwasaki, "Serpentine locomotion with robotic snakes," *IEEE Contr. Syst. Mag.* **22**(1), 64–81 (Feb. 2002).
107. M. W. Spong, S. Hutchinson and M. Vidyasagar, *Robot Modeling and Control*, New Jersey, USA (John Wiley & Sons, Inc., 2006).
108. A. A. Transeth, R. I. Leine, C. Glocker, K. Y. Pettersen and P. Liljebäck, "Snake robot obstacle aided locomotion: Modeling, simulations, and experiments," *IEEE Trans. Robot.* **24**(1), 88–104 (Feb. 2008).
109. A. A. Transeth, N. van de Wouw, A. Pavlov, J. P. Hespanha and K. Y. Pettersen, "Tracking Control for Snake Robot Joints," *Proceedings of IEEE/RSJ International Conference on Intelligent Robots and Systems*, San Diego, CA (Oct.–Nov. 2007) pp. 3539–3546.
110. A. A. Transeth, R. I. Leine, C. Glocker and K. Y. Pettersen, "3D snake robot motion: Non-smooth modeling, simulations, and experiments," *IEEE Trans. Rob.* **24**(2), 361–376 (Apr. 2008).